Eur. Phys. J. B **31**, 41–45 (2003)
DOI: 10.1140/epjb/e2003-00006-x

THE EUROPEAN PHYSICAL JOURNAL B

Raman spectroscopy of self-assembled Ge islands on Si

T.R. Yang[1,a], M.M. Dvoynenko[1], Z.C. Feng[2], and H.H. Cheng[3]

[1] Department of Physics National Taiwan Normal University 117 Taipei, Taiwan
[2] School of Electrical & Computer Engineering, Georgia Institute of Technology, Atlanta, GA 30332-0250, USA
[3] Center of Condensed Matter, National Taiwan University, 106 Taipei, Taiwan

Received 30 May 2002 / Received in final form 20 August 2002

Abstract. We present a Raman scattering study for self-organized Ge dots on Si substrate. By means of difference Raman spectroscopy technique, we have separated the Raman signals from the Ge islands and Si substrate. The wetting layer thickness and strain were estimated from the line width and peak frequency. The estimated wetting layer thickness values are comparative with the Ge dot height obtained from microscopy measurements. The strain is decreased with an increase of the thickness.

PACS. 78.30.Am Elemental semiconductors and insulators – 78.66.Db Elemental semiconductors and insulators – 63.22.+m Phonons or vibrational states in low-dimensional structures and nanoscale materials

In recent years the self-organized quantum dots have attracted much attention due to their important technological applications in nanoelectronics and photonics [1]. Raman spectroscopy is a good tool to study strains and sizes of nanostructured islands [2,3]. As regards Ge on Si substrates, however, a discussion has been raised by Kolobov and Tanaka concerning whether one can make unambiguous conclusions from the Raman spectra for Ge layers on Si substrates [4–8]. The problem lies in the presence of signals from Ge (one-phonon signal) and Si substrate (process involving two acoustic phonons) in the same frequency region. In this paper, we would show that it is possible to separate the signals from Ge dots and Si substrate, and also that one can get information about strain and thickness of Ge islands even for thin Ge layers.

The experimental samples in the present study were prepared by solid source molecular beam epitaxy (MBE) system. It consists of a buffer layer of silicon with a thickness of about 50 nm, grown on Si(001) substrate, followed by the deposition of Ge. The substrate temperature was about 300 degree. The growth rate for all samples is about 0.05 nm/s. The self-organized Ge dots were characterized by atomic force microscopy (AFM). The dots show a quasi-pyramidal shape. The average size in the growth plane was 30–40 nm for the samples N 264, N 266 and 40–50 nm for the samples N 265, N 267. The average dot height was 0.8, 1.2, 1.5 and 4.2 nm for the samples N 264, N 265, N 266 and N 267, respectively. The density of Ge islands is high. The AFM images show that the Ge islands overlap. The cross-section picture for the sample N 265 (for example) is presented in Figure 1. There is no free substrate surface without Ge. Therefore, one can consider that the Ge system is a film with changing thickness. So, the thickness of Ge layer changes from minimum thickness to maximum one (equal to minimum thickness plus dot height).

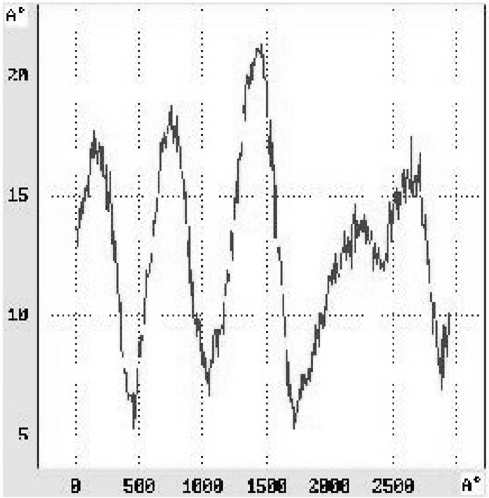

Fig. 1. Cross-section in AFM picture for the sample N 265: the behavior of the height on lateral coordinate.

The Raman spectra were measured at room temperature using a Dilor XY spectrometer with a charge-coupled device detector. The spectra were recorded in the $z(x,y)\bar{z}$ backscattering geometry. All the spectra studied were excited with the 514 nm line from an argon-ion laser. The Raman spectra are presented in Figures 2 (the samples with Ge islands) and 3 (the bulk Si and Ge), both for the

---

[a] e-mail: `yang1@scc.ntnu.edu.tw`

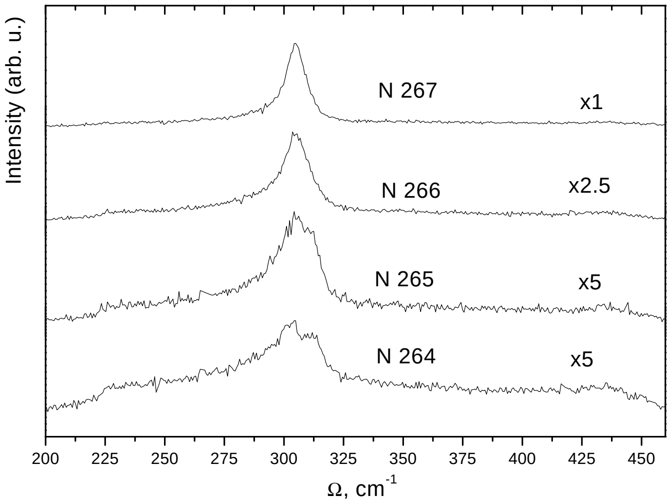

Fig. 2. Raman spectra of four samples with Ge dots grown on Si. The spectra were normalized: all amplitudes are divided by the amplitude of the principal Si substrate peak at approximately 520 cm^{-1}.

Raman shift range in wavenumber, Ω, of 200–460 cm^{-1}. To focus on the issues discussed in this study, strong Raman features from Si substrates are not displayed here. But, amplitudes of all the spectra presented in Figure 2 are divided by the amplitude of the principal Si substrate peak lying approximately at 520 cm^{-1}, *i.e.* normalized to the Si Raman signal. For the pure Si substrate one can see the known Si-Raman features at 226, 434 and 302 cm^{-1} [9]. Taking into account the dependence of the Ge phonon frequency on isotopic composition [10], we got the Raman data for the bulk Ge that was used to produce the above-mentioned dots. It is seen that the phonon frequency for our Ge material is 300 cm^{-1}. From Figure 2 one can see the difference among four spectra presented there. Because of the presence of features at 434 and 226 cm^{-1}, the Raman spectra for the samples N 264 and N 265 in Figure 2 are similar to the one for Si substrate in Figure 3. However, for these samples the main peaks in the range of 200–460 cm^{-1} are observed at frequencies of about 302 and 313 and 302 and 312 cm^{-1}, respectively. For the samples N 266 and N 267 the major peak is at a frequency about 305 cm^{-1}, and the features at 434 and 226 cm^{-1} are hard to recognize. The main peak intensity for the sample N 267 is bigger than that for other samples. It can be found that the line broadening decreases with the increase of the Ge island height and wetting layer thickness. It should be also noted that we did not observe a peak at 400 cm^{-1} associated with the Si-Ge mode [11].

An increase of the Raman signal intensity with the Ge layer thickness indicates that the signal is caused by Ge (not Si 2 TA phonon). Certainly, the presence of the weakly pronounced lines at 434 and 226 cm^{-1} indicates some contribution from the Si substrate that decreases with the Ge thickness. Indeed, our observation shows that the absolute value of the signal amplitude at the Si substrate frequency 520 cm^{-1} decreases with the Ge thickness. This fact is most pronounced for the sample N 267.

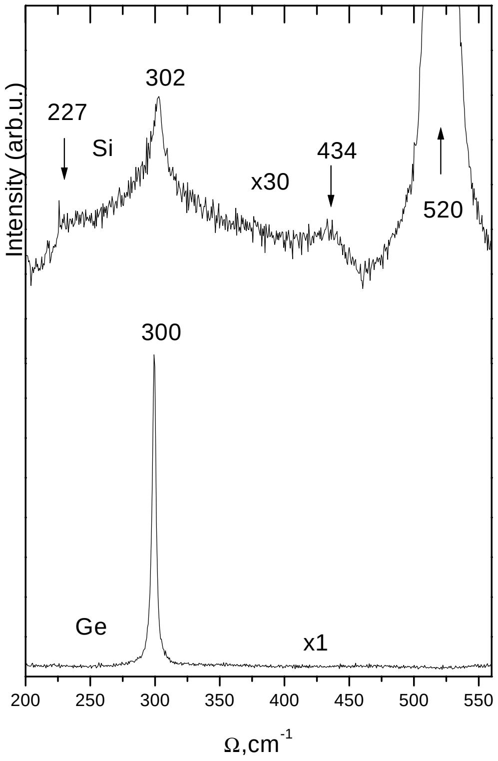

Fig. 3. Raman spectra of bulk Si and Ge. The Ge frequency peak is at 300 cm^{-1} almost, the Si two TA phonons peaks are at 302 cm^{-1}, 227 cm^{-1} and 434 cm^{-1}. The main Si peak is at 520 cm^{-1}.

Although the frequency of the main peak for the samples N 266 and N 267 is close to that of the Si Raman peak, we have to examine their origin further. Taking into account the above mentioned experimental facts and argument, one can conclude that these peaks for the samples N 266 and N 267 are caused mainly by the Ge islands and wetting layer. Let's further examine the case for the samples N 264 and N 265. How strongly do the pure Si spectra differ from that of Si used as substrate? We believe that this effect is not strong. It is necessary to take into account that the light penetration depth for a pure Si is about 300–400 nm at the wavelength of 514 nm [12]. The size of the strained region in Si substrate is equal to that of quantum dots. Therefore the Si Raman signal is associated mainly with an unstrained Si region. Indeed, our experimental data show that the principal Si peak lying at 520 cm^{-1} does not change visibly from sample to sample, as compared to the pure Si. J.L. Liu *et al.* [6], referring to the paper [13], has confirmed a fact that the intensity of the Si two acoustic phonon peak is about the same with and without strains. Therefore, to find out a signal from the Ge islands and wetting layer it is necessary to determine a difference between the complex spectra of the Ge/Si samples and those of Si.

Figure 4 shows the spectra obtained using this procedure. In this procedure, we have made the same intensity at 520 cm^{-1} for all the Ge/Si samples studied and pure Si and then, we have found a difference between the

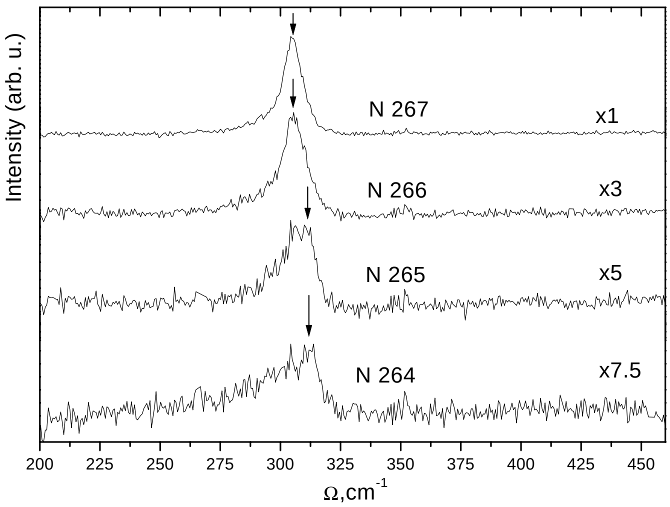

Fig. 4. The difference between the normalized Raman spectra of the samples with Ge dots (presented in Fig. 2) and Si (shown in Fig. 2). The arrows indicate the locations of the LO peak frequencies.

normalized complex spectra of the Ge/Si samples and those of Si. One can see that the features at 434 and 229 cm^{-1} disappear in such difference spectra. This fact indicates the absence of Si contribution to these spectra (as we know [9] the features at 434 and 229 cm^{-1} accompany main 2 acoustic phonon peak at 302 cm^{-1}). From Figures 2 and 4 it is found that the peaks in spectra for the samples N 266 and N 267 do not change significantly. However, as for the samples N 264 and N 265, their difference Raman spectra in Figure 4 show an essential decrease of the amplitude of the peak at 302 cm^{-1}. This peak is associated with the Si substrate two TA phonon line. The peaks at 313 cm^{-1} and 312 cm^{-1} for the samples N 264 and N 265 still exist. They are associated with optical phonons in Ge. What are features in the spectra presented in Figure 4? First, one can see that the peak frequencies are differed for all four samples. Second, all four samples have different line width. The line width decreases with increasing Ge thickness. For the samples N 264 and N 265 one can see essentially asymmetric broadened line. The asymmetric line form broadened to lower frequencies indicates (taking into account the bulk dispersion curve for optical phonons in Ge), that Raman spectra in thin Ge islands are caused by optical phonons at high values of the wavevector. This is possible for localized (or quasi-localized) phonons. Note that the 2 TA-phonons Si line has a symmetric form. Thus, a disappear of the features at 434 and 229 cm^{-1} and essentially asymmetric inhomogeneous line in the different spectra (Fig. 4) indicate the absence of Si 2 acoustic phonon contribution to them.

The higher value of the phonon peak frequencies for the Ge/Si samples, as compared to the case of bulk Ge phonon, indicates the presence of strains. Since the lattice constant of the bulk Ge is 4% higher than that of the bulk Si, the phonon frequency of Ge islands and films on the Si substrate increases. However, the possible confinement effect decreases the resonance frequency due to the dispersion curve of the Ge bulk phonon frequency, which decreases with the wave vector. The decrease of the phonon frequency (for the sample N 264 to 260–270 cm^{-1}) could be explained by the presence of Si-Ge alloy (the Ge-Ge mode in Si at low Ge concentration is 280 cm^{-1}). But in this case we would observe the Si-Ge mode (at about 400 cm^{-1}). Since there is no it, we consider the pure Ge on Si. So, these factors (strain and phonon localization) tend to change the frequency in the opposite directions. In the absence of strains the Ge optical phonons in the Brillouin zone center are triply degenerate due to the cubic symmetry of the crystal. Application of a biaxial stress in the xy plane splits the phonon degenerate frequencies into two modes (TO and LO). It should be noted that in the experimental geometry $z(x,y)\bar{z}$ of the Raman scattering LO phonons are allowed, but TO phonons are forbidden. Therefore, the main peak in Figure 4 is associated with LO phonons. This supposition (it corresponds to selection rules in bulk Ge) is confirmed by the fact that we did not observe Raman signals in the $z(x,x)\bar{z}$ experimental geometry. The directions (100) and (010) are equivalent. We shall assume that the strain xx- and yy-components are equal ($e_{xx} = e_{yy} = e$). The LO-phonon frequency shift is $\frac{\Delta\omega^{LO}}{\omega^{LO}} \approx \frac{pe_{zz}+2qe}{2\omega_0^2}$ [14]. According to the paper [3] $p = -1.46\omega_0^2$ and $q = -1.92\omega_0^2$. So $\frac{\Delta\omega^{LO}}{\omega^{LO}} \approx -0.73e_{zz} - 1.92e$. The compressive strain in the plane leads to the Ge atomic stretching along the [001] direction. Since an external force does not act along the [001] direction, one can write $\sigma_{zz} = 0$, where σ_{zz} is the zz-component of the stress tensor. From this condition one can find $e_{zz} = -\frac{2C_{12}}{C_{11}}e \approx -0.66e$ [12], where C_{12} and C_{11} are the elasticity tensor components for Ge crystal. Last expression is valid for a film. We have used it because the Ge layer is a film with slowly changing thickness. For the Ge lattice in our case the strain-induced shift for LO phonon frequency at the Brillouin zone center is $\Delta\omega^{LO} \approx -429e$ (cm^{-1}) [14,15]. It means that at any compressive strain ($e < 0$) in the growth plane the phonon frequency is increased as compared to unstrained bulk Ge. Thus, due to the compressive biaxial strain the Ge- like LO-phonon frequency can change in the region 300 cm^{-1}–317 cm^{-1}.

The maximal shift is possible when the lattice constant of Ge becomes equal to that of Si. This case corresponds to $e \approx -0.04$ and, consequently, $\Delta\omega^{LO} \approx 17$ cm^{-1}. To estimate the shift caused by the confinement effect we suggest that the strain-induced shift is the same for all the wave vector values. For a film of thickness h the frequency of a phonon localized in this film can be found from the dispersion curve. On the dispersion curve this frequency corresponds to the wave vector $q = \frac{\pi}{h}$ [16]. (We mean the first confined phonon mode: the half of the corresponding wavelength equals the film thickness). So both effects (strain and phonon localization) shift the value of the phonon frequency, but in opposite directions.

From the comparison of the peak frequency of Ge/Si with that of the Ge bulk, one can state with assurance that these Ge islands and layers are strained. We have used the following steps for finding Ge film parameters:

- from a low boundary of the Raman Ge line one finds out the minimum thickness of the Ge film (using the bulk dispersion curve of the Ge optical phonon [12] and the formula for confined phonons);
- the maximum value of the Ge thickness is determinate as the sum of the minimum thickness and the island height obtained from AFM measurement;
- obtaining confinement phonon shift for the maximum thickness (obtaining the value of the optical phonon frequency of the strained Ge at zero wave vector);
- obtaining the xx-component of the strain (e) from the value of the phonon shift at zero wavevector.

From Figure 4, one can see that all four samples have different widths of the line. The lateral size of the Ge islands is essentially bigger than their height. Different parts of the Ge film contain different integer number of Ge monolayers. The lateral sizes of the film pieces contained integer number of Ge monolayers are still essentially bigger than their thicknesses (especially for the samples N 264 and N 265). Therefore, one can consider (as first approximation) optical phonons in the Ge film pieces (bounded in the lateral directions) as in an infinity film. To analyze phonon properties of an infinity film we used the one dimension model of independent linear chains of Ge atoms directed along [001] (the one dimension model of the linear chains of atoms is considered, for example, in [17] for GaAs/AlAs superlattices). So, different points of the Ge film of variable thickness contain the chains with different length. Due to the confined phonon effect different lengths of the chains give the different frequencies. Therefore, the frequency peak (almost the higher boundary of the phonon line) corresponds to the maximum thickness, the lower boundary of the phonon line corresponds to the minimum thickness. For example, for the sample N 264 the lower boundary of phonon line is observed at 265–275 cm^{-1}. From the dispersion curve of the bulk Ge (we have used a graph taken from [12] one can find out the wavevector, and then, thickness of the wetting layer (according to the formula that connects the wavevector of a confined phonon with the thickness). We have considered as first approximation, that the dispersion curve of a strained bulk Ge can be obtained from the one of an unstrained Ge by corresponding strain induced shift. Taking into account of the strain shift of the bulk dispersion curve (approximately, 10 cm^{-1} for the samples N 264 and N 265), one can estimate an average thickness of the wetting layer (minimum thickness of the Ge film). The minimum thickness is 4–5 Å about. Note that we do not know the true strain but for very thin layers (as in the samples N 264 and N 265) a strain inexactitude influent not strongly. So the maximum thickness of the Ge film is 13 Å about. The frequency shift caused by confinement effect at the maximum thickness (13 Å) is 3–4 cm^{-1}. Therefore, the frequency at zero wavevector of the strained Ge film is 316 cm^{-1} (313+3) and, consequently, the strain in the Ge layer and islands for the sample N 264 corresponds to 4%. Analogously, one can find out the wetting layer thickness and strain for other samples. For the sample N 265 the average wetting layer thickness is 6 Å, the strain is 3.8%. The Ge layer thicknesses for the samples N 266 and N 267 are bigger than for the samples N 264 and N 265. Therefore, for the samples N 266 and N 267 the frequency shifts caused by the phonon confinement are less than that for N 264 and N 265. At the same time the differences between the peak frequencies and the bulk phonon frequency (300 cm^{-1}) for the samples N 266 and N 267 are smaller than for other samples. It is difficult to find out the minimum thickness with good precision for the samples N 266 and N 267 because of not exact determination of their line low boundaries and small slope of the dispersion curve at big thickness ($\frac{\mathrm{d}\omega}{\mathrm{d}q} = 0$ at $q = 0$). Taking the phonon localization shift 1 cm^{-1} (approximately it corresponds to the Ge thickness of about 2.5 nm) for the maximum thickness of the sample N 266, one finds the strain to be about 1.7%. For the sample N 267 with the high thickness one can not take into consideration the phonon confinement shift. The strain for this sample can be estimated from the value of the shift of the peak frequency. It is about 1.5%.

It should be noted the following. Strictly speaking the phonon localization takes place when bulk dispersion curves of neighbor semiconductors do not overlap (it is valid, for example, for GaAs/AlAs superlattices). However, the Ge LO-phonon and Si LA-phonon dispersion branches overlap. Therefore, there is possibility for propagating the Ge LO-phonons in Si substrate as LA phonons. A phonon localization degree was calculated for Si/Ge superlattices [18]. It was shown that for small phonon wavevector values the Ge LO phonons are almost localized (or quasi-localized). At the same time these phonons with high wavevector values penetrate in Si. It is clear that the Raman scattering on such phonons has lower intensity (a sign of a phonon displacement corresponds to a sign of Raman signal field). One see that the amplitude of the Raman scattering on optical phonons with a high wavevector value is less than the one for the phonons with a low wavevector value. Therefore, the wetting layer width can have lower value than we have estimated. Probably, some enhancement for observing the resonant Raman scattering by the phonons gives a high absorption coefficient in Ge. Indeed, at the wavelength 514 nm the absorption coefficient in bulk Ge is higher than the one in bulk Si in 20–40 times. Indeed, there is a correlation in Raman efficiency and absorption peaks: Raman efficiency for nondirect semiconductors (bulk Ge and Si) has a maximum by E$_1$-transition (see, *e.g.*, [19,20]. The E$_1$-transition takes place for bulk Ge at 2.2 eV and bulk Si at 3.5 eV. Probably this fact allows to observe Ge optical weakly localized phonons (due to "bad" resonator) with the high value of their wave vector. Also, it should be noted that for the sample N 266 and especially N 267 the lateral size of the above mentioned film pieces is not essentially bigger than their height. Therefore, the one dimension model of the independent linear chains can be applied to these samples with reservations. Probably, the phonon modes observed in Raman spectra for these samples may not be described with the use of so simple model. Therefore, we have estimated the strains for the samples N 266 and N 267, in fact, omitting the phonon confinement effect. Such estimations (without considering the phonon localization) were carried out, for example, in the papers [3,15,23].

Furthermore, the strain in the Ge layers decreases with thickness. Therefore, maybe, the Ge quantum dots with bigger sizes are unstrained. In particular, Kolobov *et al.* [21] reported that the Ge islands on Si substrate are unstrained. These islands were about 180 nm in diameter and about 12 nm in height.

Let us now further examine whether it is possible to separate the signals from the islands and wetting layer or not. Liu *et al.* [6] reported that they could discriminate the signals from wetting layer and dots using the selection rules. We would like to stress that one should be very careful to apply the selection rules to the nanostructured objects. The field inside and outside of a particle is inhomogeneous and can change its direction (see, for example, the field distribution in triangles in the paper [21]. One could say the same about the wetting layer because its thickness is approximately equal to the size of quantum dots placed on this layer. These effects are associated with a near optical field and depend on the particle shape and other parameters. These effects can be the reason for an observation of TO phonons in the geometry $z(x,y)\bar{z}$ or $z(x,x)\bar{z}$ (see *e.g.*, [3]). Therefore, there seem to be no complete and valid evidences to confirm the above use of the selection rules in the case of nanostructured objects to be correct (the weakening of the selection rules in Ge/Si superlattices with Ge quantum dots, see, for example, in [22].

In conclusion we have performed a Raman scattering study for the self-organized Ge dots formed on Si substrates. By means of the difference Raman techniques, we have separated the Raman signals of the Ge-islands and wetting layer from the pure Si. The average wetting layer thickness and strain were estimated from frequency peak and line width.

References

1. D. Bimberg, M. Grundmann, N.N. Ledentsov, *Quantum Dot Heterostructures* (Wiley, Chichester, United Kingdom, 1998)
2. Z.M. Jiang, C.W. Pei, X.F. Zhou, W.R. Jiang, B. Shi, X.H. Liu, Xung Wang, Q.J. Jia, W.L. Zheng, X.M. Jiang, Appl. Phys. Lett. **75**, 370 (1999)
3. A.B. Talochkin, V.A. Markov, A.I. Nikiforov, S.A. Tits, JETP Lett. **70**, 288 (1999)
4. A.V. Kolobov, J. Appl. Phys. **87**, 2926 (2000)
5. A.V. Kolobov, K. Tanaka, Appl. Phys. Lett. **75**, 3572 (1999)
6. J.L. Liu, Y.S. Tang, K.L. Wang, Appl. Phys. Lett.**75**, 3574 (1999)
7. A.V. Kolobov, K. Tanaka, Appl. Phys. Lett. **78**, 3550 (2001)
8. A.K. Das, J. Kamila, B.N. Dev, B. Sundaravel, G. Kuri, Appl. Phys. Lett. **78**, 3552 (2001)
9. P.A. Temple, C.E. Hathaway, Phys. Rev. B **7**, 3685 (1973)
10. J.M. Zhang, M. Giehler, A. Gobel, T. Ruf, M. Cardona, Phys. Rev. B **57**, 1348 (1998)
11. M.I. Alonso, K. Winer, Phys. Rev. B **39**, 10056 (1989)
12. *Semiconductors: Group IV Elements and III-V Compounds*, edited by O. Madelung (Springer-Verlag, Berlin, 1991)
13. J.-M. Baribeau, D.J. Lockwood, T.E. Jackman, P. Aebi, T. Tyliszczak, P. Hitchcock, Can. J. Phys. **69**, 246 (1991)
14. F. Cerdeira, C.J. Buchenauer, F.H. Pollak, M. Cardona, Phys. Rev. B **5**, 580 (1972)
15. A. Milekhin, N.P. Stepina, A.L. Yakimov, A.I. Nikiforov, S. Schulze, D.R.T. Zahn, Eur. Phys. J. B **16**, 355 (2000)
16. T. Dumelow, T.J. Parker, S.R.P. Smith, D.R. Tilley, Surf. Sci. Rep. **17**, 151 (1993)
17. B. Samson, T. Dumelow, A.A. Hamilton, T.J. Parker, S.R.P. Smith, D.R. Tilley, C.T.B. Foxon, D. Hilton, K.J. Moore, Phys. Rev. B **46**, 2375 (1992)
18. A. Fasolino, E. Molinari, J.C. Maan, Phys. Rev. B **39**, 3923 (1989)
19. R. Schorer, G. Abstreiter, H. Kibbel, H. Presting, Phys. Rev. B **50**, 18211 (1994)
20. A.B. Talochkin, S.P. Suprun, A.V. Efanov, I.G. Kozhemyako, V.N. Shumskii, JETP Lett. **73**, 337 (2001)
21. A.V. Kolobov, H. Oyanagi, K. Brunner, P. Schittenhelm, G. Abstreiter, K. Tanaka, Appl. Phys. Lett. **78**, 451 (2001)
22. J.P. Kottmann, O.J. Martin, D.R. Smith, S. Schultz, New J. Physics **2**, 27 (2000)
23. A.G. Milekhin, A.I. Nikiforov, O.P. Pchelyakov, S. Schultze, D.R.T. Zahn, JETP Lett. **73**, 461 (2001)